California Current Acidification Network (C-CAN)
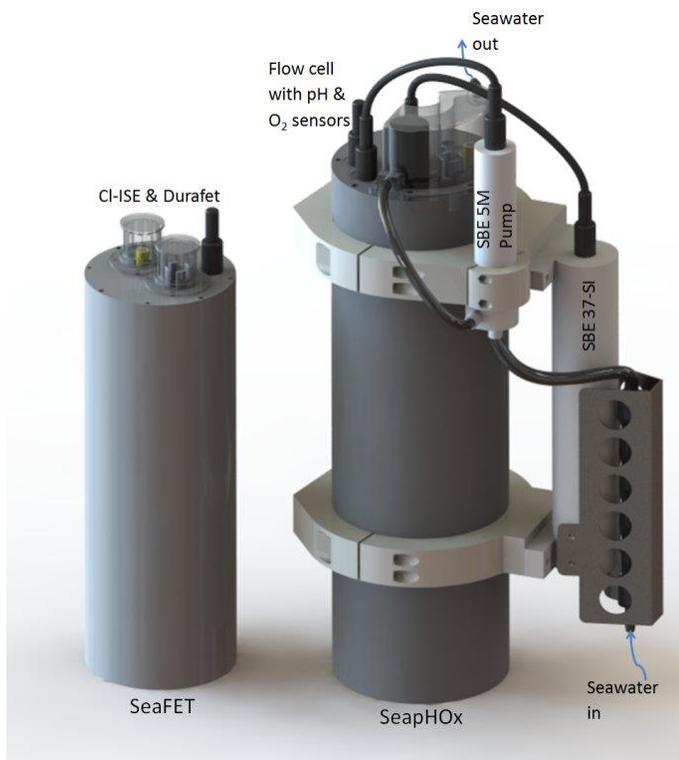

Best Practices for autonomous measurement of seawater pH with the Honeywell Durafet pH sensor

Todd Martz, Karen McLaughlin, Stephen B. Weisberg

March 2015

Contents

Acknowledgements

C-CAN Steering Committee Members
Stephen Weisberg (Chair), *Southern California Coastal Water Research Project Authority*
Debbie Aseltine-Neilson, *California Department of Fish and Game*
Alan Barton, *Pacific Coast Shellfish Grower's Association*
Sue Cudd, *Whiskey Creek Shellfish Hatchery*
Andrew Dickson, *Scripps Institution of Oceanography*
Richard A. Feely, *NOAA Pacific Marine Environmental Laboratory*
Ian W. Jefferds, Penn Cove Shellfish
Libby Jewett, *National Oceanic and Atmospheric Administration*
Teri King, *University of Washington*
Chris Langdon, *Oregon State University*
Skyli McAfee, *California Ocean Science Trust*
Jan Newton, *University of Washington*
Bruce Steele, California sea urchin diver

C-CAN Methods Committee Members

Todd Capson, *Sustainable Fisheries Partnership*
Burke Hales, *Oregon State University*
Dwight Gledhill, *NOAA Ocean Acidification Program*
Joseph Salisbury, *University of New Hampshire*
Simone Alin, *NOAA Pacific Marine Environmental Laboratory*
Alan Barton, *Whiskey Creek Shellfish Hatchery*
Benoit Eudeline, *Taylor Shellfish Hatchery*
Andrew Dickson, *Scripps Institution of Oceanography*

This report is available on the C-CAN website:

http://c-can.msi.ucsb.edu/c-can-documents

Recommended citation:
Martz, T., K. McLaughlin, S.B. Weisberg. 2015. Best Practices for autonomous measurement of seawater pH with the Honeywell Durafet pH sensor. California Current Acidification Network (C-CAN).

Preface

The California Current Acidification Network (C-CAN) is a collaboration dedicated to advancing understanding of ocean acidification (OA) and its effects on biological resources of the U.S. West Coast. C-CAN first convened in 2010 in response to a growing realization that declines in shellfish hatchery production corresponded to coastal upwelling of low pH waters. The initial workshop brought together leading shellfish industry representatives, coastal managers, researchers, Sea Grant programs, and Integrated Ocean Observing Systems to increase collective understanding of OA effects on the nearshore environment. C-CAN has since expanded to include other ocean-dependent industries, environmental advocacy groups, regulatory agencies, and tribal groups.

The overarching goal of C-CAN is to coordinate and standardize OA measurement and data collection practices, ensuring data accessibility, utility, and application. C-CAN provides shared guidelines and support for participating groups in implementation of high quality, compatible monitoring programs. C-CAN also facilitates application of the network's data in developing tools that examine the causes of ecosystem impacts and predict future changes in ocean chemistry and biological communities. Finally, C-CAN communicates its findings to address management concerns about defining the ecological effects of OA for development of mitigation and adaptation strategies. Given the complexity of this emerging issue, and recognizing that advancing knowledge will require a concerted community effort, C-CAN is committed to serve as the region's source of reliable, vetted scientific information on ocean acidification.

Introduction

Coastal ecosystems are vulnerable to ecological and biogeochemical perturbations from ocean acidification (OA) (Doney et al. 2009, Howarth et al. 2011). However, determining the effects of OA on nearshore ecosystems, including coastal and estuarine waters, is difficult due to the interplay of numerous factors including freshwater inputs, tidal forcing, water stratification, nutrient over-enrichment, algal blooms, and hypoxia (Fabry et al. 2008, Borges and Gypens 2010). Understanding the impacts of OA in the coastal environment requires coordination of monitoring efforts to ensure that intercomparable data on OA and its effects on nearshore ecosystems are collected. The California Current Acidification Network (C-CAN) was initiated, in part, to address these issues. C-CAN has developed a vision that lowers barriers to making seawater CO_2 measurements of sufficient quality to understand ecosystem effects of changing ocean chemistry[1]. One of C-CAN's core monitoring principles is that seawater OA measurements should facilitate determination of aragonite saturation state (Ω) and a complete description of the carbonate system (McLaughlin et al. 2014). This requires direct measurement of at least two carbonate system parameters, of which seawater pH is considered a master variable for understanding the impacts of OA on coastal ecosystems.

Ion Sensitive Field Effect Transistor (ISFET) pH sensors have been found to be stable and accurate for monitoring fine-scale changes in pH in open ocean environments (Le Bris and Birot 1997, Martz et al. 2010) and are becoming widely-accepted for open ocean and nearshore monitoring of high frequency variability in pH (Hofmann et al. 2011, Kroeker et al. 2011, Yu et al. 2011). However, to date there have been no broadly agreed upon best practices for deployment of such sensors. C-CAN's efforts to develop a coordinated monitoring program documenting changing ocean chemistry have led to a growing number of non-specialist users who are adopting ISFET sensors for continuous, autonomous measurement of pH in a variety of settings, exposing a need for coordinated best practices for deployment of ISFET sensors and data quality assurance and quality control. Clearly defined best practices for deployment of ISFET sensors is critical for assessing data quality and intercomparability across users, which is crucial to interpreting data from a network of sites.

The purpose of this document is to provide broadly applicable recommended protocols for autonomous pH sensors incorporating the Honeywell Durafet (based on the published work of Bresnahan et al., 2014). The Honeywell Durafet pH sensor is a commercially available and widely used sensor, which has been deployed in a variety of configurations by different users. The recommendations in this document evolved from sensor deployments carried out in various locations since 2009.

Recommendations are summarized below and a brief discussion of each point is provided on the following pages. Recognizing that not all recommendations can be practically met, the primary recommendation for all sensor users is embodied in the final protocol regarding error reporting.

---

[1]   More information on C-CAN's vision can be found in a companion document available at: http://c-can.msi.ucsb.edu/c-can-documents/C-CAN%20%20Vision%20Document%20Final.pdf/view)

Recommended Protocols

1. Preceding deployment, operate sensors in natural seawater until initial sensor drift due to conditioning ends (approx. 5-10 days), with daily samples in order to observe the pre-deployment conditioning period; repeat this process following deployment for validation. Power the ISFET continuously during this period.
2. Collect a careful shore-side calibration point based on discrete sample(s) following the conditioning period.
3. Store sensors in seawater between deployments.
4. Prevent biofouling as permitted, especially within the euphotic zone.
   i. Utilize an actively flushed flow scheme that minimizes light.
   ii. Incorporate a Sea-Bird instrument with tributyltin plugs into the flow scheme.
   iii. Wrap sensor housings with tape (McMaster-Carr P/N 6029T98) and paint with EP-SN1 or similar antifouling paint.
   iv. When using passively flushed SeaFET sensors, incorporate a 70:30 Cu-Ni alloy tube into a flow stream around Durafet and ISE.
5. When practical, take frequent discrete samples alongside a sensor throughout a deployment in order to establish an error estimate in the sensor data. At minimum collect one bottle sample alongside an operating deployed sensor.
6. Deploy co-located, independent sensors such as redundant pH, pCO$_2$, and O$_2$ sensors.
7. Estimate pH from regional empirical and/or thermodynamic relationships.
8. Assess and control pH sensor data quality with discrete pH and estimated pH using the following plots:
   i. *time-series anomaly* to first identify and then eliminate periods of ostensible sensor conditioning, drift, and failure.
   ii. *property-property* to examine agreement between sensor pH and an independent reference pH (through the intercept, c_0, & slope, c_1). Property-property plots are useful for quality assessment; that is, a c_0 significantly different from 0 and/or c_1 from 1 indicates bias in the sensor and/or reference pH used for comparison.
9. Apply a single calibration point, chosen to minimize the anomaly relative to a trustworthy reference pH throughout the deployment. In particular, it is not recommended to force sensor data to agree with multiple individual bottle samples as this imparts sampling error to the sensor time series.
10. Establish an error envelope for the sensor time-series. The accuracy of the sensor time-series can be no better than the reference to which it is calibrated or validated.

About the sensors

Ion Sensitive Field Effect Transistor (ISFET) pH sensors can be deployed in a variety of configurations. This set of guidelines is based on experience with the "SeaFET" design (commercialized by Satlantic, L.P.), which consists of a Honeywell Durafet and a solid-state chloride ion selective electrode (Cl-ISE) (Martz et al., 2010), though many of these recommendations apply broadly to other ISFET and glass electrode pH sensors.

Unlike potentiometric glass electrodes, the ISFET sensor is an active electronic device, based on Metal Oxide Semiconductor Field Effect Transistor (MOSFET) technology. When exposed to solution, the oxide

coating of the MOSFET's conduction channel exchanges protons (hydrogen ions), giving rise to an interface potential that is measured as a voltage between the source of the MOSFET and a reference electrode. For further details the reader is referred to Bergveld (2003). In the SeaFET, the ISFET voltage is recorded relative to two independent reference electrodes: an internal Ag/AgCl reference with a liquid junction and a junctionless external Cl-ISE, referred to hereafter as E_{INT} and E_{EXT}, respectively (Martz et al., 2010).

The pH of seawater is calculated from the measured sensor voltage using the Nernst equation to relate sensor voltage to hydrogen ion concentration. Corresponding pH values for the internal and external reference electrodes, pH^{INT} and pH^{EXT}, are derived from the internal and external voltages respectively, the temperature of the solution, and a calibration constant (termed "E0" in Note 2 below, E* in Bresnahan et al., (2014), and sometimes referred to as K0, or E^o). A single-point calibration, specific to each reference electrode, defines the intercept (E0) in a line of pH vs. sensor voltage at the in situ calibration conditions. Thus, the calibration point is specified as a sensor voltage at a particular pH, temperature, and salinity. Sensor voltages are extended over a range of pH, temperature, and salinity by assuming a 100% Nernst slope and that the relative change in voltage with temperature is constant. The reader is referred to Note 2 and Bresnahan et al. (2014) for equations and further details.

The dual reference electrode design is not a requirement, but can aid in evaluating data quality. Due to the difficulty of achieving a stable potentiometric reference (Culberson, 1981), the two independent reference electrode design provides a theoretical improvement due to the fact that the liquid junction potential of the internal reference is unquantifiable and therefore adds uncertainty to the pH_{INT} value, an uncertainty that can be evaluated with the external reference (Martz et al., 2010). However, experience has also shown that the internal reference electrode is of the highest quality and, under many circumstances, appears to remain nearly as stable as the external reference. Consequently, retaining two reference electrodes provides a simple check during data QC: differences between pH_{INT} and pH_{EXT} serve as an indicator of sensor malfunction and/or fouling. However, users should be cautioned, due to the unmeasurable liquid junction potential, pH_{INT} has a poorly characterized (yet small) salinity response that leads to increasing errors as salinity departs from that at the time of calibration. Although this error in pH_{INT} is presumed to be small over narrow salinity ranges, this may not be the case if there are large salinity variations. The thermodynamic uncertainty due to the liquid junction potential cannot be ignored when the sensor is deployed in coastal locations with significant freshwater input or large temperature variability. However, in test tank experiments over the salinity range 30-36, an effect on the liquid junction potential could not be identified and therefore a salinity correction for the pH_{INT} under typical seawater conditions is not recommended (Bresnahan et al., 2014).

Discussion of Recommended Protocols

Recommendation 1. Preceding deployment, operate sensors in natural seawater until initial sensor drift from sensor conditioning ends (approx. 5-10 days).

When first placed in seawater, pH sensor voltages relative to both reference electrodes exhibit an asymptotic drift (Figure 1). This conditioning period is due to several factors: 1) the time required to achieve a stable flow of ions across the liquid junction of the internal reference electrode (nominally hours), 2) the time required to replace chloride ions with bromide ions in the solid solution of AgCl in the

Cl-ISE (nominally days), 3) the time required for an ISFET conditioning component, related to the initial power-up of the chip, the exact basis of which is not fully understood (nominally 1 day), and 4) a pressure effect on the ISFET and internal reference electrode through changes in the liquid junction potential that may become important if the sensor is deployed more than ~20 m below the surface (nominally 1 hour). Factors 1-3 can be addressed by operating the pH sensor continuously in seawater (never powering off the ISFET) for one week prior to deployment and taking care to keep the sensor wetted in natural seawater during transport. If these preconditioning procedures are ignored, the sensor may exhibit drift during the first days of a deployment. The fourth aspect of conditioning (a pressure effect) is problematic to characterize as it appears to be sensor specific and not necessarily repeatable. Using the Durafet sensor for profiling applications in the 0-80 m range (rated depth) is therefore discouraged. However, Durafets have been successfully operated at 80 m for extended periods; the key to a successful deployment rests in selecting an appropriate reference pH once the sensor is deployed and conditioned at depth.

As a result of these experiments, best practices should include pre-deployment operation of Durafet sensors in natural seawater until the initial sensor drift due to conditioning is finished (approx. 5-10 days). Furthermore, daily samples of discrete pH should be collected in order to observe the pre-deployment conditioning period; a process which should be repeated following deployment for validation. The ISFET should be powered continuously during this period and throughout the deployment.
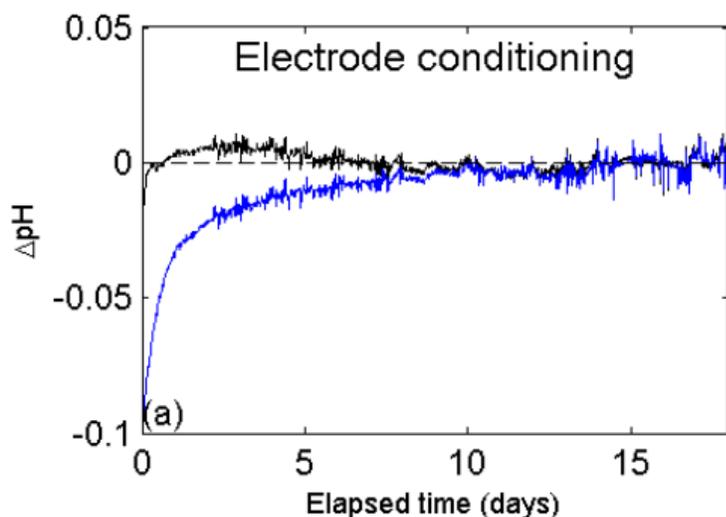

Figure 1 (From Breshahan et al, 2014, Figure 5a). Time series anomaly of difference between pH measured by internal reference electrode pH^{INT} (black) and external reference electrode pH^{EXT} (blue) compared to continuous measurements of pH measured by a continuous underway spectrophotometric pH system. Black dashed lines represent a zero anomaly. Asymptotic drift at the start of each deployment to zero anomaly represents the conditioning period for each reference electrode.

Recommendation 2. Best practices require a careful shore-side calibration point based on discrete sample(s) following the conditioning period.

Whether or not sensors are factory-calibrated, we recommend checking the calibration or establishing a new calibration point on shore before deployment. The initial accuracy of a stable sensor is limited by the calibration approach. Trust in pre- and postcalibrations (i.e., setting calibration constants before sensors are deployed or after they are recovered) of any marine chemical sensor relies on two hard to satisfy criteria: 1) sensors must be calibrated in a similar physical setting (i.e., similar temperature,

salinity, pressure) to that of the study location and 2) sensors must not undergo significant (re)conditioning in their new environments (See Recommendation 1). It is always preferred to rigorously calibrate a sensor before deployment, but this may require facilities and time that are not available. Honeywell provides an initial factory calibration of every Durafet sensor on the NBS pH scale, but provides no statement of calibration accuracy or stability, recommending that the user perform the canonical NBS buffer standardization employed widely for all glass electrodes. Because the NBS pH scale is not recommended for seawater pH measurements (Marion et al., 2011), at minimum, the Honeywell Durafet must be recalibrated on the appropriate pH scale (C-CAN recommends use of the total hydrogen ion scale, see Note #1) before use in oceanographic applications. Due to these complications, it is recommended that the user calibrate an operating Durafet to a discrete measurement of pH taken shore-side after the sensor is conditioned. This practice also serves to validate laboratory calibration. The calibration sample must coincide in time and space with the comparison sensor measurement.

Matlab code is provided at the conclusion of this document (Note 2) to enable a user to derive calibration coefficients for the internal and external reference electrodes (**pHCalib.m)** and utilize those calibration coefficients to calculate pH from the measured time-series voltages on each electrode during deployment (**pHCalc.m)**.

Recommendation 3. Store sensors in seawater between deployments.

Following initial conditioning period (Recommendation 1), sensors should be transported to the deployment site and maintained in natural seawater between deployments to minimize potential reconditioning, and associated sensor drift, in a new environment. Although placing a sensor in a low ionic strength solution such as freshwater or standard buffers will not damage the sensor, the sensor may condition to these solutions if placed in them, requiring reconditioning once placed in a saline environment. The sensor should be also be powered continuously during the time following conditioning in order to avoid the warm-up period associated with powering ON the ISFET sensor.

Recommendation 4. Prevent biofouling as permitted, especially within the euphotic zone.

Biofouling is the leading cause of measurement error in the nearshore environment, dominating the time series anomaly signal on the weekly to monthly timescales (Figure 2). Thus prevention of biofouling is critical in these environments. The approach to biofouling prevention has been evolving as experience with the in situ Durafet sensor grows and is expected to continue to improve. Presently, to minimize biofouling, it is recommended that users utilize an actively flushed flow scheme that minimizes light, such as that incorporated into the SeapHOx configuration. Actively flushed (i.e., pumped) sensor packages show far greater stability than passively flushed packages, with the former remaining stable in a wide variety of environments on timescales approaching one year, and the latter often succumbing to biofouling within one month. Below the euphotic zone, the flushing scheme appears to be less important, with both packages remaining stable for greater than nine months. In addition, incorporation of a Sea-Bird instrument with tributyltin biocide plugs into the flow scheme is also recommended. Sensor housings should be wrapped with tape (McMaster-Carr P/N 6029T98) and painted with EP-SN1 or similar antifouling paint. The enclosures block most light, which not only reduces biofouling, but also mitigates the direct impact of light on sensor response, which can be substantial for an ISFET. If the user is deploying a passively flushed SeaFET sensor, it is recommended that they incorporate a 70:30 Cu-Ni

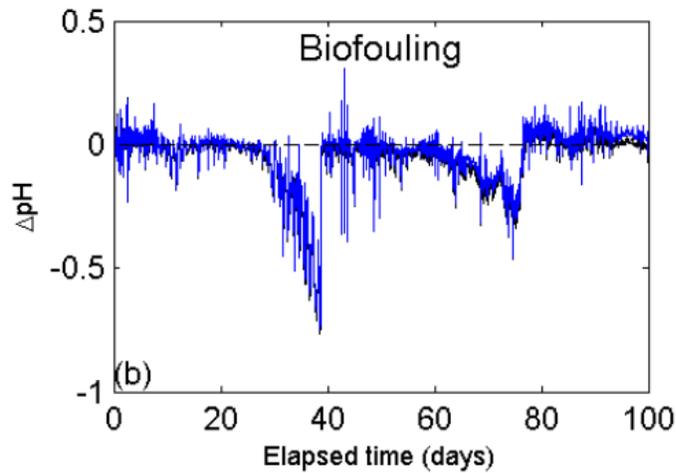alloy tube into a flow stream around the Durafet and ISE, which has proven superior to the original Cu mesh.

Figure 2 (From Breshahan et al, 2014, Figure 5b). Time series anomaly of difference between pH measured by the internal reference electrode pH^{INT} (black) and external reference electrode pH^{EXT} (blue) compared to continuous independent measurements of pH from the internal pH reference electrode of a stable co-deployed SeapHOx sensor package on a mooring. Black dashed lines represent a zero anomaly.

Recommendation 5. When practical, take frequent discrete samples alongside a sensor throughout a deployment in order to establish an error estimate in the sensor data.

Several factors that affect the ideal bottle sampling frequency include length of deployment, access to study site, rate of fouling, availability of co-located sensors, and access to real-time data. For example, it may be helpful to collect weekly bottle samples for an easily accessed sensor in a high fouling environment, while open ocean locations may be limited to bottle measurements at the time of deployment and recovery.

As noted above, pH sensor measurements are ideally calibrated with a single E0 that minimizes the difference between trustworthy, discrete pH measurements, assessed using standard bench top procedures (Dickson et al., 2007) and the sensor measurements. Frequent, discrete measurements should be collected to both establish an error estimate for the sensor time series, as well as to identify when the sensor data become suspect due to fouling, sensor drift or battery failure. Discrete measures of pH serve as an independent sensor validation point(s) following initial calibration and care should be taken when using discrete measurements to apply corrections to sensor data during post-processing (see recommendation 9).

Recommendation 6. Deploy co-located, independent sensors such as redundant pH, pCO2, and O2 sensors.

Although not a requirement, co-located sensors can augment a time-series in ways that bottle samples cannot. Sensor redundancy provides a powerful cross check for discerning data quality. Comparison of two independent measures of pH, or a variable that is expected to co-vary with pH such as dissolved oxygen or pCO_2, can help to identify sensor problems such as the onset of fouling. Without independent validation based on bottle samples (per Recommendation 5), additional sensors, or post-calibration, the output of any sensor must be skeptically viewed. Simply put, in a situation where a single pH electrode

(ISFET, glass, etc.) is deployed with a single reference electrode in the absence of additional biogeochemical sensors or discrete samples to provide data quality control, the resulting pH time-series should be viewed as unsubstantiated. We acknowledge that these requirements add complexity to sensor deployments but suggest that the returns in data quality are worth the effort. The Durafet sensor packages offer resolution that can't practically be matched by discrete sampling programs and have gained popularity due to their ease of use and low cost. Investment in a redundant pH sensor, or co-location with a dissolved oxygen or pCO_2 sensor will insure data quality, and in the case of oxygen and pCO_2 sensors will provide additional biogeochemical contextual data for analysis.

Recommendation 7. Estimate pH from regional empirical and/or thermodynamic relationships.

Co-located chemical sensors can be used to derive empirical pH values which can then be used in lieu of measured pH data to evaluate sensor performance and characterize sensor malfunction and/or drift. These relationships are regional in nature and must therefore be calibrated to each new area and re-evaluated over time. For example, Alin et al. (2012) report several empirical relationships between pH, pCO_2, O_2, temperature, and salinity. In combination with relationships such as these, thermodynamic equations from the program CO2SYS for Matlab (van Heuven et al., 2011) can be used to derive an estimated pH. Most commonly, regional relationships for estimating total alkalinity as a function of temperature and salinity, TA^{est}, are combined with co-located pCO_2 sensor data to estimate pH from pCO_2 and total alkalinity. Combining the error in TA^{est} (6.4 $\mu mol \cdot kg^{-1}$ as defined by Alin et al. 2012) and pCO_2 (less than 5 μatm), the propagated error in the estimated pH would be less than 0.01 pH units using CO2SYS (Bresnahan et al. 2014).

Figure 3 demonstrates how use of a co-located dissolved oxygen sensor and the regional algorithm for estimating pH from Alin et al. 2012 was used to identify drift in the internal reference electrode. The internal and external reference electrodes began to deviate from one another after 100 days of deployment, use of the oxygen sensor to estimate pH enabled identification of the external reference electrode as providing accurate pH data. Without the oxygen data, it would have been impossible to pinpoint the source of pH sensor drift between the ISFET, internal reference, and external reference electrode. The drift in pH^{INT} relative to pH^{EXT} would have signaled a problem with the system and both pH values would have been flagged as 'bad.'
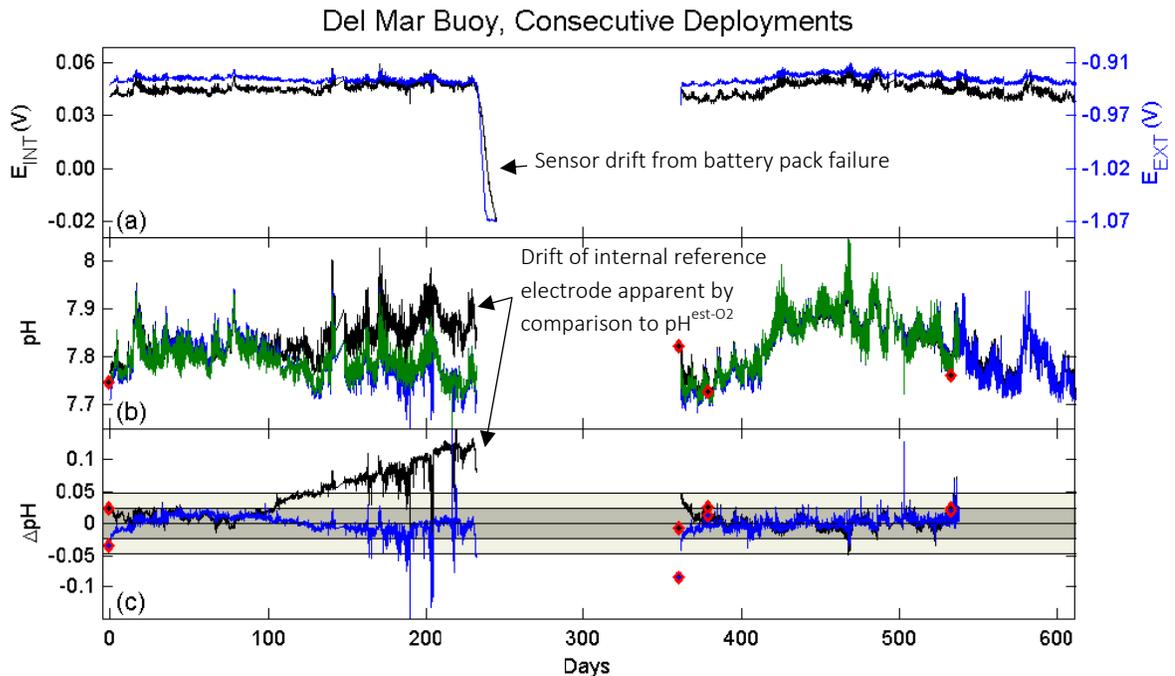
Figure 3 (From Breshahan et al, 2014, Figure 2). Del Mar Buoy pH time-series beginning on 25-Jun-2011. (a) Raw sensor voltages for internal (black) and external (blue) reference electrodes show two consecutive deployments with a four-month gap. (b) pH is calculated using the internal (pH^{INT}, black) and external (pH^{EXT}, blue) reference electrodes and estimated from oxygen and temperature (pH^{est_O2}, green). Discrete sample values are black diamonds with red edges. (c) Anomalies (ΔpH) for pH^{INT} (black) and pH^{EXT} (blue) are shown relative to pH^{est_O2} (solid lines) and discrete samples (filled diamonds, red edges) with σ (dark gray) and 2σ (light gray) shaded regions, where standard error in pH^{est_O2} as reported by Alin et al. (2012) is 0.024 pH units. The optode failed on 15-Dec-2012 but the SeaFET functioned until 28-Feb-2013, leaving the pH time-series without a pH^{est_O2} value for the last 75 days.

Recommendation 8. Assess and control pH sensor data quality with discrete pH and estimated pH using the time-series anomaly and property-property plots.

Time-series anomaly plots, wherein the time-series of the differences between sensor pH and an independent assessment of pH are shown, can be used to first identify and then eliminate periods of ostensible sensor conditioning, drift, and failure. pH anomalies are reported as ΔpH^{i-j} where i and j refer to two independent measures (or empirical estimate(s)) of pH. Time-series anomaly plots act as a screening tool for acceptable data.

Similarly, property-property plots can be used to examine agreement between sensor pH and an independent, reference pH. Sensor offset (i.e., intercept, c_0), and slope (c_1), relative to an independent, reference pH value (pH estimated from discrete samples, pH estimated from O_2, or pH estimated from pCO_2) can be calculated from a Model II least squares fit (Peltzer, 2007) of property-property plots (namely, pH_{sensor} vs. $pH_{reference}$). Property-property plots are useful for quality assessment; that is, a c_0 significantly different from 0 and/or c_1 significantly different from 1 indicates bias in the sensor and/or

reference pH used for comparison. Examples of property-property plots are given below in Figure 4. Note that when computing a c_0, to assess the presence of sensor offset, it may be preferable to scale the regression equation to the observed range of pH values such that the lowest values measured correspond to the graphical origin (i.e., in Figure 4a, $y = c_0 + c_1x$ becomes $y = 8.1 + c_0' + (x-8.1)c_1$. Thus, the c_0' value and its associated error better reflect sensor performance over the range of values observed by the instrument.
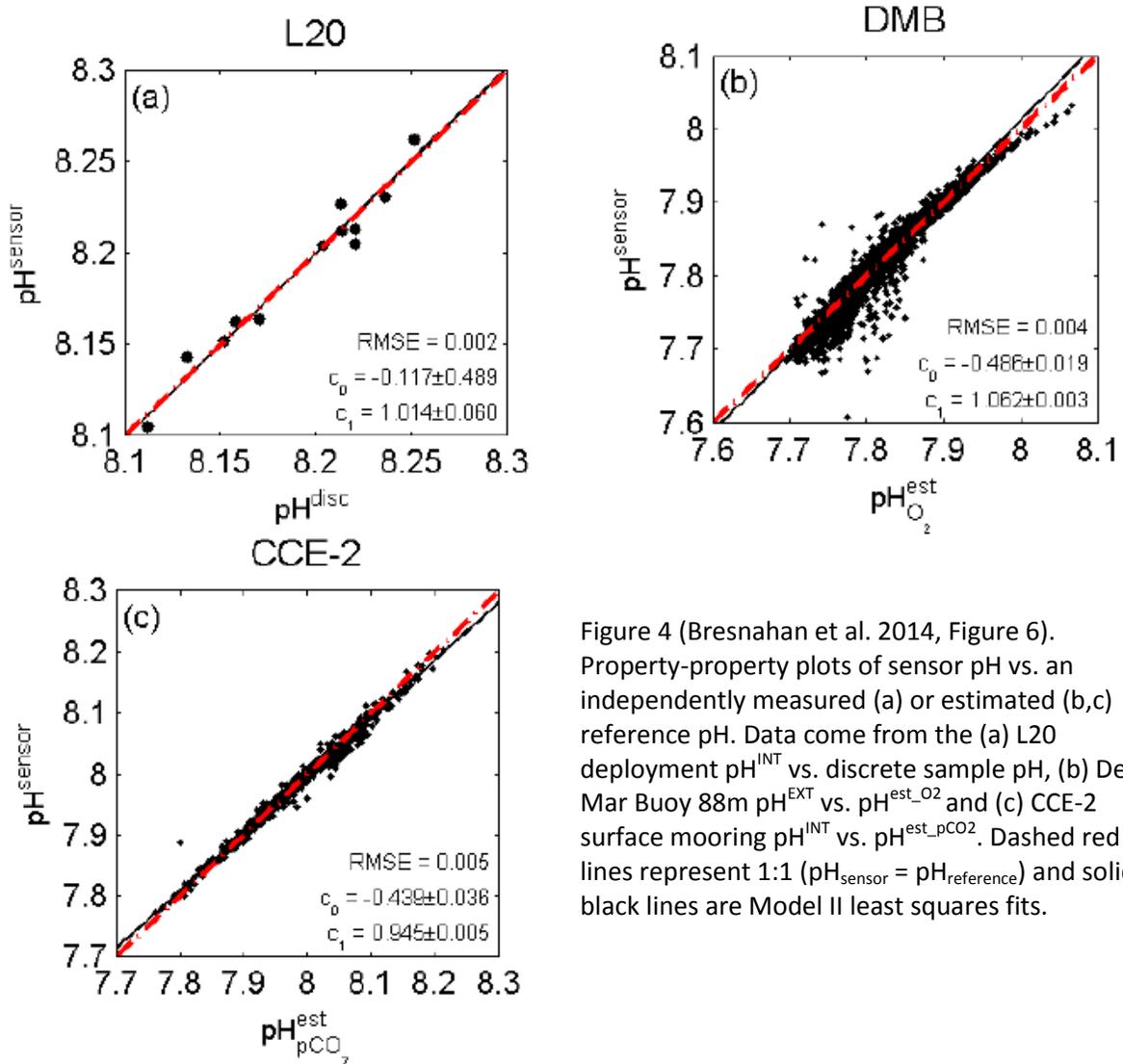

Figure 4 (Bresnahan et al. 2014, Figure 6). Property-property plots of sensor pH vs. an independently measured (a) or estimated (b,c) reference pH. Data come from the (a) L20 deployment pH^{INT} vs. discrete sample pH, (b) Del Mar Buoy 88m pH^{EXT} vs. pH^{est_O2} and (c) CCE-2 surface mooring pH^{INT} vs. pH^{est_pCO2}. Dashed red lines represent 1:1 ($pH_{sensor} = pH_{reference}$) and solid black lines are Model II least squares fits.

Recommendation 9. Apply a single calibration point, chosen to minimize the anomaly relative to a trustworthy reference pH throughout the deployment. In particular, it is not recommended to force sensor data to agree with multiple individual bottle samples as this imparts sampling error to the sensor time series.

In addition to the pre-deployment calibration, we recommend incorporating validation samples into an ongoing sensor deployment. These samples serve to validate the pre-deployment calibration, identify sensor drift or failure, and potentially correct sensor data in the event of calibration drift.

Experience indicates that the Durafet remains stable over multiple months when deployed continuously in seawater. The Durafet sensors repeatedly demonstrate a 100% Nernstian response (Takeshita et al., 2014) and exhibit a stable and repeatable potential at a given temperature, salinity, and pH, with a highly linear and stable response to temperature across multiple sensors. This long-term sensor stability justifies a single-point calibration approach under most circumstances. The single-point calibration, specific to each reference electrode, defines the intercept (E_0) in a line of pH vs. sensor voltage at in situ calibration conditions. Thus, the calibration point is defined as a sensor voltage at a known pH, temperature, and salinity. Sensor voltages are extended over a range of pH, temperature, and salinity by assuming a 100% Nernst slope and a constant rate of change in voltage with temperature. For a thorough description of the various pH scales and inter-conversions, the reader is referred to Marion et al. (2011). Users are discouraged from forcing sensor data to agree with multiple individual bottle samples taken over the time course as this has been demonstrated to impart sampling error to the sensor time series. An in situ calibration point should be taken after period of initial conditioning (if conditioning of sensor was not conducted prior to deployment) and within the first week of deployment before any discernable sensor drift has occurred.

In physically and biogeochemically dynamic environments such as the nearshore, it can be challenging to capture synchronized discrete samples to set an accurate calibration constant. At the site where the data from Figure 5 were collected (MBARI L20 mooring), the SeapHOx sensors observed average pH changes of 0.023 pH·hr^{-1} but recorded instantaneous rates at least a full order of magnitude greater; thus, calibrating to a sample with even slight spatiotemporal mismatch in such an environment can introduce significant errors (Bresnahan et al. 2012). As opposed to using a single data point, Breshnahan et al., used a calibration constant for a SeapHOx which forced the mean difference between the sensor values and discrete values to be zero, thus minimizing the overall difference between sensor and discrete samples of pH. Figure 5 depicts the resulting offsets for each individual discrete measurement and the sensor value that results when E0 is set using an average value to minimize the differences in pH between the internal and discrete pH measurements. This anomaly resulted from: (1) significant environmental pH gradients combined with small spatiotemporal mismatch between sensor and discrete sample and/or (2) errors in the discrete sample analysis. Analysis of the time-series suggested that spatiotemporal mismatch is the dominant control; in a dynamic near-shore ecosystem, a small sampling discrepancy could certainly contribute (unbiased) anomalies of this magnitude. The random anomalies in Figure 5 suggests that resetting the calibration constant to match each discrete value would impart an artificial variability in calculated pH with a magnitude of ~0.015 pH units and a frequency equal to the discrete sampling frequency. By choosing a single calibration constant based on multiple discrete samples, the error is substantially reduced.

In summary, best practices suggest first eliminating sensor data with identifiable drift using a time-series anomaly plot followed by correcting data to more reliable contemporaneous pH measurements. If and only if the reference pH is trustworthy, E0 is calculated such that the average anomaly between sensor and reference is minimized.
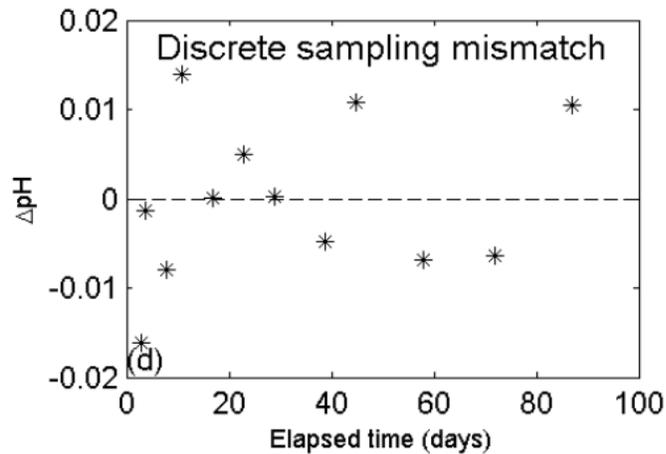
Figure 5 (From Breshahan et al, 2014, Figure 5d). Time series anomaly of difference between pH measured by the internal reference electrode pH^{INT} of a SeapHOx compared to independent, discrete measurements of pH measured in the laboratory using the *m*-cresol purple spectrophotometric method. Black dashed lines represent a zero anomaly.

Recommendation 10. Establish an error envelope for the sensor time-series. The accuracy of the sensor time-series can be no better than the reference to which it is calibrated or validated.

Without an estimate of the error associated with each of the measurements, comparisons of datasets across regions and time are meaningless. Thus, the final recommendation is to establish and report the error envelope for each sensor deployment. Report errors as RMSE between sensor and reference values.

Note 1: pH Scale

For data reporting purposes a pH scale must be specified. The pH is commonly calculated on the free, total (tot), and seawater (SWS) scales. A pH value, reported on a particular scale is converted to another scale as follows:

$$pH_{tot} = pH_{free} - \log\left(1 + \frac{S_T}{K_S}\right)$$

$$pH_{tot} = pH_{SWS} - \log\left(1 + \frac{S_T}{K_S}\right) + \log\left(1 + \frac{S_T}{K_S} + \frac{F_T}{K_F}\right)$$

$$pH_{SWS} = pH_{free} - \log\left(1 + \frac{S_T}{K_S} + \frac{F_T}{K_F}\right)$$

$$pH_{SWS} = pH_{tot} + \log\left(1 + \frac{S_T}{K_S}\right) - \log\left(1 + \frac{S_T}{K_S} + \frac{F_T}{K_F}\right)$$

$$pH_{free} = pH_{tot} + \log\left(1 + \frac{S_T}{K_S}\right)$$

$$pH_{free} = pH_{SWS} + \log\left(1 + \frac{S_T}{K_S} + \frac{F_T}{K_F}\right)$$

where S_T, F_T, K_S, K_F are functions of temperature and salinity. Further details on these calculations may be found in (Riebesell et al., 2010) and recommended software programs include CO2SYS (Lewis and Wallace, 1998) and CO2calc (Robbins et al., 2010)

For ease of comparability, C-CAN recommends that all pH data be reported on the total scale.

Note 2: Data processing functions for sensors based on the Honeywell Durafet

The functions below are provided for users with access to raw voltages from Durafet-based sensors. Durafet users without access to raw voltages may still follow the recommended protocols listed above, by processing all data in the pH domain.

getDurafetTemp.m returns temperature (tempC, °C) from the Durafet's thermistor voltage (VTherm, V) when an independent conductivity/temperature sensor is not available. Note that Durafet thermistors are accurate to ±0.5 °C, making it necessary to perform a calibration to a known reference temperature in order to retrieve an offset value (TCOffset, °C).

```
function tempC = getDurafetTemp(VTherm,TCOffset)
% Convert Durafet thermistor voltage to temperature (C) using following
polynomial
c0 = 340.9819863; c1 = -9.10257E-05; c2 = -95.08806667; c3 = 0.965370274;
RTherm = 20000./(3.3./VTherm-1);
tempC = c0+c1*RTherm+c2*log10(RTherm)+c3*(log10(RTherm)).^3;
tempC = tempC+TCOffset;
```

pHCalib.m has inputs of discrete E_{INT} (V), E_{EXT} (V), pH, temperature (°C), and salinity at time of calibration and returns the calibration coefficients $E_{INT,25}^*$ and $E_{EXT,25}^*$.

```
function calib = pHCalib(calEint,calEext,calpH,calT,calsal)
% Univ gas constant, Faraday constant,
R = 8.3145; F = 96487;
% Temperature dependence of standard potentials, Martz et al. 2010
dE0int = -0.001101; dE0ext = -0.001048;
% See Martz et al. 2010 for greater detail
tempK = calT+273.15; % Convert temp from C to K
S_T = (R*tempK)/F*log(10); % Nernst temp dependence
E0int = calEint-S_T*calpH; % Calc E0int from Nernst & pH @ calibration point
E0int25 = E0int+dE0int*(25-calT);
Z = 19.924.*calsal./(1000-1.005.*calsal); % Ionic strength, Dickson et al.
2007
SO4_tot = (0.14/96.062)*(calsal./1.80655);  % Total conservative sulfate
cCl = 0.99889/35.453.*calsal/1.80655; % Conservative chloride
mCl = cCl*1000/(1000-calsal.*35.165/35); % mol/kg-H2O
K_HSO4 = exp(-4276.1/tempK+141.328-23.093*log(tempK)...
         +(-13856/tempK+324.57-47.986*log(tempK))*Z^0.5...
         +(35474/tempK-771.54+114.723*log(tempK))*Z-2698/tempK*Z^1.5...
         +1776/tempK*Z^2+log(1-0.001005.*calsal)); % Bisulfate equilibrium
const., Dickson et al. 2007
pHint_free = calpH+log10(1+SO4_tot/K_HSO4);
cHfree = 10^(-pHint_free); % mol/kg-sw
pHint_free = pHint_free+log10((1000-calsal.*35.165/35)/1000); % mol/kg-H2O
mHfree = 10^(-pHint_free); % mol/kg-H2O
DHconst = 0.00000343*calT^2+0.00067524*calT+0.49172143; % Debye-Huckel, Khoo
et al. 1977
log10gamma_HCl = 2*(-DHconst*sqrt(Z)/(1+1.394*sqrt(Z))+(0.08885-
0.000111*calT)*Z);
```

```
aHfree_aCl = mHfree*mCl*10^(log10gamma_HCl);
E0ext = calEext+S_T*log10(aHfree_aCl);
E0ext25 = E0ext+dE0ext*(25-calT);



calib = [E0int25 E0ext25];
```

pHCalc.m uses the calibration coefficients to calculate pH given the full E_{INT}, E_{EXT}, temperature, and salinity time-series. Note that the term E0 written in the code below is referred to as E* in text and what is here written as E (*e.g.*, E_{INT}, E_{EXT}) has often been referred to in its engineering units as V (V_{INT}, V_{EXT}).

```
function calc = pHCalc(Eint,Eext,E0int25,E0ext25,tempC,salt)
% Univ gas constant, Faraday constant,
R = 8.3145; F = 96487;
% Temperature dependence of standard potentials, Martz et al. 2010
dE0Int = -0.001101; dE0Ext = -0.001048;
% See Martz et al. 2010 for greater detail
tempK = tempC+273.15; % Convert temp from C to K
S_T = (R*tempK)/F*log(10); % Nernst temp dependence
pHint_tot = (Eint-(E0int25+dE0Int*(tempC-25)))./S_T; % Calc pHint from Nernst
Z = 19.924.*salt./(1000-1.005.*salt); % Ionic strength, Dickson et al. 2007
SO4_tot = (0.14/96.062).*(salt./1.80655); % Total conservative sulfate
cCl = 0.99889./35.453.*salt./1.80655; % Conservative chloride
mCl = cCl.*1000./(1000-salt.*35.165/35); % mol/kg-H2O
K_HSO4 = exp(-4276.1./tempK+141.328-23.093.*log(tempK)...
        +(-13856./tempK+324.57-47.986.*log(tempK)).*Z.^0.5...
        +(35474./tempK-771.54+114.723.*log(tempK)).*Z-
2698./tempK.*Z.^1.5...
        +1776./tempK.*Z.^2+log(1-0.001005.*salt)); % Bisulfate equilibrium
const., Dickson et al. 2007
pHint_free = pHint_tot+log10(1+SO4_tot./K_HSO4); % free scale mol/kg-sw
DHconst = 0.00000343.*tempC.^2+0.00067524.*tempC+0.49172143; % Debye-Huckel,
Khoo et al. 1977
log10gamma_HCl = 2*(-DHconst.*sqrt(Z)./(1+1.394*sqrt(Z))+(0.08885-
0.000111*tempC).*Z);
pHext_free = -(((E0ext25+dE0Ext*(tempC-25))-Eext)-
S_T.*(log10(mCl)+log10gamma_HCl))./S_T; % mol/kg-H2O
pHext_free = pHext_free-log10((1000-salt.*35.165/35)/1000); % mol/kg-sw
pHext_tot = pHext_free-log10(1+SO4_tot./K_HSO4);

calc = [pHint_tot pHext_tot];
```

References

Alin, S. R., R. A. Feely, A. G. Dickson, J. M. Hernández-Ayón, L. W. Juranek, M. D. Ohman, and R. Goericke (2012), Robust empirical relationships for estimating the carbonate system in the southern California Current System and application to CalCOFI hydrographic cruise data, *J. Geophys. Res.*, *117*(C5), C05033.

Bergveld, P., 2003. Thirty years of ISFETOLOGY: What happened in the past 30 years and what may happen in the next 30 years. Sensors Actuators B Chem. 88, 1–20. doi:10.1016/S0925-4005(02)00301-5

Borges, A.V., and Gypens , N. 2010 Carbonate chemistry in the coastal zone responds more strongly to eutrophication than to ocean acidification. Limnol. Oceanogr. 55, 346-353.

Bresnahan, P., T. R. Martz, Y. Takeshita, K. S. Johnson, and M. LaShomb (accepted), Best Practices for autonomous measurement of seawater pH with the Honeywell Durafet.

Byrne, R.H., Degrandpre, M.D., Short, R.T., Martz, T.R., Merlivat, L., McNeil, C., Sayles, F.L., Bell, R., Fietzek, P., 2009. Sensors and Systems for In Situ Observations of Marine Carbion Dioxide System Variables. OceanObs'09.

Clayton, T.D., Byrne, R.H., 1993. Spectrophotometric seawater pH measurements: total hydrogen ion concentration scale calibration of m-cresol purple and at-sea results. Deep Sea Res. Part I Oceanogr. Res. Pap. 40, 2115–2129. doi:10.1016/0967-0637(93)90048-8

Culberson, C., 1981. Direct potentiometry, in: Whitfield, M., Jagner, D. (Eds.), Marine Electrochemistry: A Practical Introduction. pp. 187–262.

Cullison Gray, S.E., DeGrandpre, M.D., Moore, T.S., Martz, T.R., Friederich, G.E., Johnson, K.S., 2011. Applications of in situ pH measurements for inorganic carbon calculations. Mar. Chem. 125, 82–90. doi:10.1016/j.marchem.2011.02.005

Dickson, A.G., Sabine, C.L., Christian, J.R. (Eds.), 2007. Guide to Best Practices for Ocean CO2 Measurements, PICES Spec. ed.

Doney, S. C., Fabry, V. J., Feely, R. A., & Kleypas, J. A., 2009. Ocean acidification: the other CO2 problem. Oceanography 22: 36-47.

Easley, R.A., Patsavas, M.C., Byrne, R.H., Liu, X., Feely, R.A., Mathis, J.T., 2013. Spectrophotometric measurement of calcium carbonate saturation states in seawater. Environ. Sci. Technol. 47, 1468–77. doi:10.1021/es303631g

Emerson, S., Sabine, C., Cronin, M.F., Feely, R., Cullison Gray, S.E., DeGrandpre, M., 2011. Quantifying the flux of CaCO3 and organic carbon from the surface ocean using in situ measurements of O2, N2, pCO2, and pH. Global Biogeochem. Cycles 25, GB3008. doi:10.1029/2010GB003924

Frieder, C.A., Nam, S.H., Martz, T.R., Levin, L.A., 2012. High temporal and spatial variability of dissolved oxygen and pH in a nearshore California kelp forest. Biogeosciences 9, 3917–3930. doi:10.5194/bg-9-3917-2012

Friederich, G.E., Brewer, P.G., Herlien, R., Chavez, F.P., 1995. Measurement of sea surface partial pressure of C02 from a moored buoy. Deep Sea Res. Part I Oceanogr. Res. Pap. 42, 1175–1186. doi:10.1016/0967-0637(95)00044-7

Fabry, V. J., Seibel, B. A., Feely, R. A., and Orr, J. C. 2008. Impacts of ocean acidification on marine fauna and ecosystem processes. – ICES Journal of Marine Science, 65: 414–432.

Hofmann, G.E., Smith, J.E., Johnson, K.S., Send, U., Levin, L.A., Micheli, F., Paytan, A., Price, N.N., Peterson, B., Takeshita, Y., Matson, P.G., Derse Crook, E., Kroeker, K.J., Cristina Gambi, M., Rivest, E.B., Frieder, C.A., Yu, P.C., Martz, T.R., 2011. High-frequency dynamics of ocean pH: a multi-ecosystem comparison. PLoS One 6. doi:10.1371/journal.pone.0028983

Howarth, R., Chan, F., Conley, D. J., Garnier, J., Doney, S. C., Marino, R., & Billen, G., 2011. Coupled biogeochemical cycles: eutrophication and hypoxia in temperate estuaries and coastal marine ecosystems. Frontiers in Ecology and the Environment, 9(1), 18-26.

Johnson, K.S., Jannasch, H.W., Coletti, L.J., Carlson, R., Brown, G., Nohava, T., Martz, T.R., Takeshita, Y., Swift, D., Riser, S.C., 2013. Towards a global ocean pH observing system: First observations with Deep-Sea Durafet pH sensors on profiling floats, in: ASLO Aquatic Sciences Meeting. New Orleans, LA.

Khoo, K.H., Ramette, R.W., Culberson, C.H., Bates, R.G., 1977. Determination of hydrogen ion concentrations in seawater from 5 to 40 degrees C: standard potentials at salinities from 20 to 45 per mil. Anal. Chem. 49, 29–34. doi:10.1021/ac50009a016

Kline, D.I., Teneva, L., Schneider, K., Miard, T., Chai, A., Marker, M., Headley, K., Opdyke, B., Nash, M., Valetich, M., Caves, J.K., Russell, B.D., Connell, S.D., Kirkwood, B.J., Brewer, P., Peltzer, E., Silverman, J., Caldeira, K., Dunbar, R.B., Koseff, J.R., Monismith, S.G., Mitchell, B.G., Dove, S., Hoegh-Guldberg, O., 2012. A short-term in situ CO_2 enrichment experiment on Heron Island (GBR). Sci. Rep. 2, 413. doi:10.1038/srep00413

Hofmann, G. E., Smith, J. E., Johnson, K. S., Send, U., Levin, L. A., Micheli, F., ... & Martz, T. R. (2011). High-frequency dynamics of ocean pH: a multi-ecosystem comparison. PloS one, 6(12), e28983.

Le Bris, N., & Birot, D., 1997. Automated pH-ISFET measurements under hydrostatic pressure for marine monitoring application. Analytica chimica acta, 356(2-3), 205-215.

Lewis, E. and D. Wallace (1998), Program developed for CO2 system calculations, DOE, ORNL/CDIAC-105.

Liu, X., Patsavas, M.C., Byrne, R.H., 2011. Purification and characterization of meta-cresol purple for spectrophotometric seawater pH measurements. Environ. Sci. Technol. 45, 4862–8. doi:10.1021/es200665d

Liu, X., Wang, Z.A., Byrne, R.H., Kaltenbacher, E.A., Bernstein, R.E., 2006. Spectrophotometric measurements of pH in-situ: laboratory and field evaluations of instrumental performance. Environ. Sci. Technol. 40, 5036–44. doi:10.1021/es0601843

Marion, G.M., Millero, F.J., Camões, M.F., Spitzer, P., Feistel, R., Chen, C.-T.A., 2011. pH of seawater. Mar. Chem. 126, 89–96. doi:10.1016/j.marchem.2011.04.002

Martz, T.R., Connery, J.G., Johnson, K.S., 2010. Testing the Honeywell Durafet for seawater pH applications. Limnol. Oceanogr. Methods 8, 172–184. doi:10.4319/lom.2010.8.172

Martz, T.R., Send, U., Ohman, M.D., Takeshita, Y., Bresnahan, P.J., Kim, H.-J., Nam, S., 2014. Dynamic variability of biogeochemical ratios in the Southern California Current System. Geophys. Res. Lett. 41, 2496–2501. doi:10.1002/2014GL059332

McLaughlin, K., S.B. Weisberg, A. Dickson, G. Hofmann, J. Newton. 2013. Core Principles for Development of a West Coast Network for Monitoring Marine Acidification and Its Linkage to Biological Effects in the Nearshore Environment. California Current Acidification Network (C-CAN).

Peltzer, E., 2007. Model II least squares fit: lsqfitma.m, http://www.mbari.org/staff/etp3/regress/lsqfitma.m.

Riebesell, U., Fabry, V.J., Hansson, L., Gattuso, J.-P. (Eds.), 2010. Guide to best practices for ocean acidification research and data reporting. Publications Office of the European Union, Luxembourg.

Robbins, L.L., Hansen, M.E., Kleypas, J.A., and Meylan, S.C., 2010, CO2calc—A user-friendly seawater carbon calculator for Windows, Max OS X, and iOS (iPhone): U.S. Geological Survey Open-File Report 2010–1280, 17 p.

Sarmiento, J.L., Gruber, N., 2006. Ocean Biogeochemical Dynamics. Princeton University Press, Princeton, NJ.

Seidel, M.P., DeGrandpre, M.D., Dickson, A.G., 2008. A sensor for in situ indicator-based measurements of seawater pH. Mar. Chem. 109, 18–28. doi:10.1016/j.marchem.2007.11.013

Takeshita, Y., T. R. Martz, K. S. Johnson, and A. G. Dickson. 2014. Characterization of an Ion Sensitive Field Effect Transistor and Chloride Ion Selective Electrodes for pH Measurements in Seawater. Anal. Chem. 86: 11189-11195.

Van Heuven, S., Pierrot, D., Rae, J.W.B., Lewis, E., Wallace, D.W.R., 2011. MATLAB Program Developed for CO2 System Calculations. doi:10.3334/CDIAC/otg.CO2SYS_MATLAB_v1.1

Yu, P.C., Matson, P.G., Martz, T.R., Hofmann, G.E., 2011. The ocean acidification seascape and its relationship to the performance of calcifying marine invertebrates: Laboratory experiments on the development of urchin larvae framed by environmentally-relevant pCO2/pH. J. Exp. Mar. Bio. Ecol. 400, 288–295. doi:10.1016/j.jembe.2011.02.016